Carbohydrate Polymers 86 (2011) 226–230

Contents lists available at ScienceDirect

Carbohydrate Polymers

journal homepage: www.elsevier.com/locate/carbpol

Studies on properties of electrospinning nanofibers of biodegradable tercopolymers derived from ε-CL, TMC and LLA

Junhua Wang, Fengchun Dong, Gang Huang, Yongtang Jia*

College of Textile and Clothing, Wuyi Universtiy, Guangdong 529020, China

ARTICLE INFO

Article history:
Received 22 March 2011
Received in revised form 13 April 2011
Accepted 15 April 2011
Available online 22 April 2011

Keywords:
Tercopolymer
Electrospinning
Nanofibers
Biodegradability

ABSTRACT

Scanning electron microscopy (SEM), diffraction scanning calorimetry (DSC), and X-ray diffraction (XRD) techniques were employed to characterize nanofiber structure and morphology. The properties of nanofibers including the mechanical property and the thermal behavior, especially biodegradability, were investigated. Due to stretching and molecular chain orientation in electrospinning process, the T_g, T_m and W_c of the nanofibers were higher than that of the corresponding tercopolymers. The T_g, T_m and W_c of the nanofibers decreased with increasing TMC content in copolymers. The mechanical properties of nanofibers changed with the different feed molar ratio. The degree of degradation of nanofibers was faster than that of the corresponding copolymers. In addition, the degradation behavior of nanofibers also altered with the different feed molar ratio. The data obtained would provide more details for application of tercopolymer nanofibers in biomedical field.

1. Introduction

Electrospinning is a convenient method which can produce ultrafine fibers with diameters ranging from micron scales to nanometers through high electric field (Aussawasathien, Teerawattananon, & Vongachariya, 2008). The resulted electrospun fibers have such characteristics as high porosity, large surface area to volume ratio and flexibility for surface functionalization, which make them have potential applications in medical areas such as tissue engineering scaffolds, immobilized enzymes and catalyst systems, wound dressing, artificial blood vessels, materials for the prevention of postoperative-induced adhesions, and so forth (Jia & Dong, 2010; Shen et al., 1997; Yoo & Park, 2009). Numerous biodegradable materials have been electrospun into nanofibers and demonstrated their potential as medical materials candidates (Lee & Jeong, 2009; Rujitanaroj & Pimpha, 2008)

Recently, nanofibers of biodegradable aliphatic polymers are receiving more and more attention (Zhu & Pitt, 1991). Among those aliphatic polyesters, much interest has been concentrated on PCL, PTMC, PLLA, PPDO, PGA as well as their copolymers (Duda & Biela, 1998; Jia & Shen, 2008; Middleton & Tipton, 2000; Narayan & Park, 2003). Xie and Wang (2006) developed PLGA-based nanofibers as implants for the sustained delivery of paclitaxel to treat C6 glioma in vitro. Li prepared copolymer nanofibers of PLA/PGA, characterized the nanofibers structure and investigated cell adhesion on nanofibers (Li & Cato, 2002). Laleh manufactured PCL/gelatin nanofibrous scaffolds for nerve regeneration (Laleh & Molamma, 2008). These studies demonstrate that nanofibers with special properties can be obtained by selecting a combination of components and adjusting the ratio of the constituents to meet the needs of different biomedical uses. Encouraged by the advantages of copolymers, a series of the tercopolymers derived from LA, ε-CL and TCM with different feed molar ratio were synthesized to develop a new family of biodegradation polymers in our previous work. The optimum reaction conditions of tercopolymers were obtained (Jia & Shen, 2008). Meanwhile the corresponding electrospun nanofibers were prepared and characterized, and the most suitable eletrospun process has been gotten. In addition, the properties of the tercopolymers and nanofibers including the thermal behavior and the crystallinity were also studied (Jia & Dong, 2010).

For biomedical materials, the biodegradability is one of the important properties. The different materials have their own different degradation. The degradation rate of PCL, PTMC is much slower than that of PLLA (Han, Branford-White, & Zhu, 2010). Biodegradability can also be tailored with the desired effects just as mentioned above by selecting different monomers copolymerization. Tsuji and Fay investigated the biodegradability of CL/LA copolymer, showing that the degradation rate of PCL increased due to adding LLA (Fay & Linossier, 2006; Tsuji & Ikada, 1998). To select the suitable biodegradable scaffolds for different biomedical applications, Kwangsok fabricated nanofibers of PLA-based multi-component blends containing two bridging materials PLA-b-PEG-b-PLA triblock copolymer and PLGA random copolymer (Kim and Yu, 2003). To gain more details for application

* Corresponding author. Tel.: +86 0750 3296413.
E-mail address: yongtjh@163.com (Y. Jia).

0144-8617/$ – see front matter © 2011 Published by Elsevier Ltd.
doi:10.1016/j.carbpol.2011.04.037

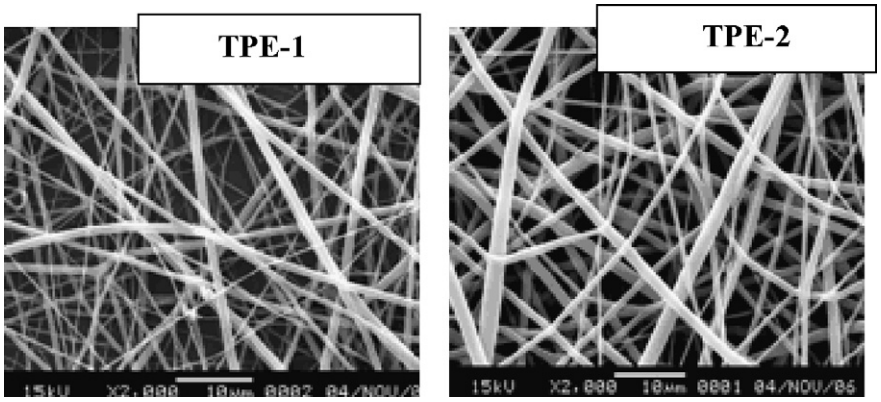

Fig. 1. SEM of TPE-1 and TPE-2.

of ε-CL/TMC/LLA tercopolymer nanofibers in biomedical field, nanofibers of tercopolymers were prepared. The properties, especially the biodegradability, were investigated preciously in this paper.

2. Experimental

2.1. Materials

Tercopolymers with molar ratio of TMC/LLA/CL of 10/50/40 (TP1) and 20/40/40 (TP2) were prepared in our previous work. Dimethyl formamide (DMF), methylene chloride (MC) were used as received.

2.2. Film preparation

The films were prepared by casting a MC solution of the tercopolymer at a concentration of 10–15 wt% on the surface of a polytetrafluorethylene film. The films of tercopolymer were dried under atmospheric temperature for 1 day, and then, were dried under vacuum at room temperature for another day.

2.3. Nanofiber preparation

The various electrospinning parameters, such as solvent, the tercopolymer concentration, the voltage and the tip-collector distance (TCD), were investigated detailedly in our previous work (Jia & Dong, 2010). The obtained optimum conditions for electrospinning nanofibers were: solvent DMF/MC = 40/60 (molar ratio), 30% copolymer concentration, 12 kV voltage and TCD 12 cm. According to the optimum conditions, nanofibers of copolymer TP1 and TP2 were fabricated (nanofibers of TP1 and TP2 are designated hereafter as TPE-1 and TPE-2 respectively). The average diameters of TPE-1 and TPE-2 were 367 nm and 395 nm. Fig. 1 is SEM photos of TPE-1 and TPE-2.

2.4. Biodegradation

Nanofibers of tercopolymers were put into sample vials with 100 ml phosphate buffer solution (pH = 7.4), which was thermostatically controlled at 37 ± 1 °C. And then, the samples were took out regularly and characterized.

2.5. Characterizations

The structure, morphology and average diameter of fibers were characterized by SEM (JSM-5600LV, JEOL Ltd.). DSC measurements were carried out on a thermal analyzer (TA) Instrument (DSC2010) (TA Instruments Ltd., New Castle, USA) covering −60 to 250 °C, in a nitrogen atmosphere at a heating rate of 10 °C min^{-1}. XRD powder patterns of the nanofibers were recorded with a Rigaku Dmax-II X-ray diffractometer using nickel-filtered Cu Kα radiation at 40 kV and 50 mA in the 2θ ranges of 4° to 40°. The mechanical properties were tested on a Shinkch Testing Machine at a cross-head speed of 20 mm min^{-1} at room temperature. Viscosity was measured with an Ubbelodhe Capillary Viscometer (Cannon Company, Pittsburgh, USA), thermostatically controlled at 25 °C. Intrinsic viscosity ([η]) was calculated by the 'One Point Method' and expressed in dl/g:

$$[\eta] = [2 \times (\eta_{sp} - \ln \eta_r]^{1/2} c$$

where $\eta_r = \eta/\eta_0$ and $\eta_{sp} = \eta_r - 1$, η and η_0 being the viscosity of the polymer solution and that of the solvent, respectively (0.1 g dl^{-1} concentration).

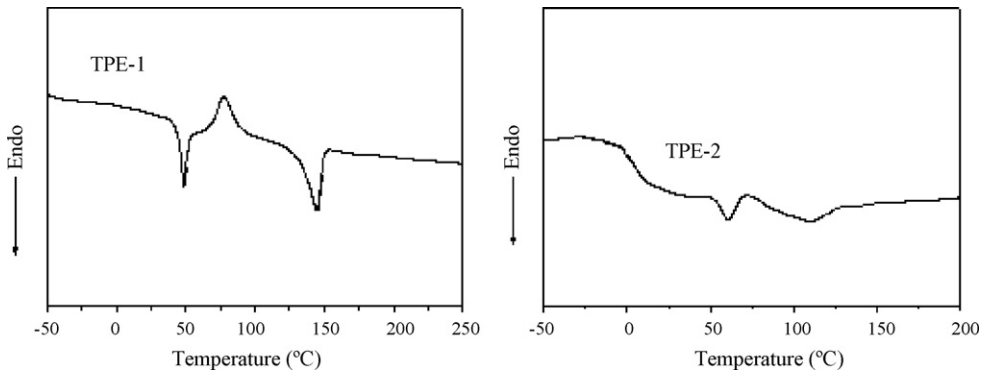

Fig. 2. DSC curves of TPE-1 and TPE-2.

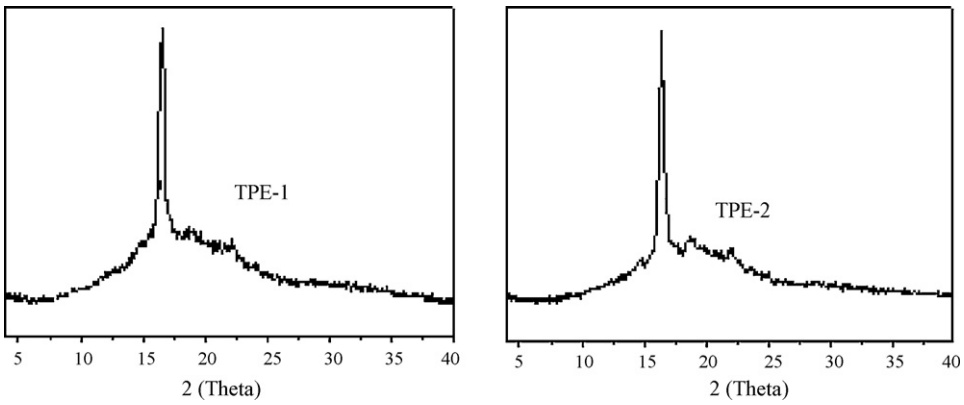

Fig. 3. XRD spectra of TPE-1 and TPE-2.

3. Results and discussion

3.1. DSC and XRD analysis

Fig. 2 shows the DSC curves of TPE-1 and TPE-2. Two melting points and a crystal exothermal peak were observed in the DSC curves of nanofibers. The phenomena were similar to those observed by Zong and Kim (2002) during electrospinning of PLLA. Appearance of the crystal exothermal peak may be due to polymer chain orientation in electrospinning.

The higher melting point was confirmed to be the crystal melting point of the tercopolymer PLLA sequence. The reason was that the higher melting point (144.78 °C) approached the melting point of pure PLLA (150–160 °C). Then, how to explain the lower melting point? The lower melting point approached the melting temperature of the PCL sequence in the copolymer, which was probably considered to be the melting temperature of the PCL sequence. However, there was no PCL crystal peak found in the XRD spectra (Fig. 3). In addition, the experiments carried out by Zong et al., focused on PLLA electrospinning. Therefore, the low temperature crystal melting peak was assigned to another crystal melting peak of a PLLA block in the tercopolymer formed during electrospinning. It is proposed that the crystal defects in the fractional PLLA block were greater and the crystal nucleus was thin during the electrospinning process, which led to a lower melting temperature.

From Table 1, it was observed that T_g, T_m, and W_c (results calculated from $W_c = \Delta H_m/\Delta H_o$ where ΔH_o of PLLA is 93.1 J/g, and ΔH_o of PCL is 142 J/g) (Kricheldorf & Kreiser-Saunders, 1995) of the nanofibers were all higher than that of corresponding tercopolymer films. This phenomenon was similar to that previously observed (Jia & Kim, 2006). During the electrospinning process, the molecular chain orientation improved and more molecules existed in crystal state with increasing the fiber elongation ratios. Thus, the T_g, T_m, and W_c increased relatively.

Table 1
DSC data of TPE-1 and TPE-2.

Samples	T_g (°C)	T_{m_1} (°C)	T_{m_2} (°C)	W_{c_1} (%)	W_{c_2} (%)
TPE-1	16.3	48.7	144.78	8.9	21.2
TP1	14.7	–	142.27	–	–
TPE-2	5.2	61.15	110.47	1.9	2.9
TP2	2.0	58.33	106.23	–	1.9

It also can be seen in Table 1 that T_g, T_m, and W_c of TPE-1 were higher than that of TPE-2. The reason lied in the different feed molar ratio of monomers in copolymers. It is well known that PTMC is an amorphous or low-crystalline polymer with low T_g, while PLLA is semi-crystalline with high T_g. The TMC content in TPE-2 was higher than that of the TPE-1, and the LLA content was inverse, which made them comply with the above rules.

3.2. The mechanical property

The mechanical property is one of the important performances for nanofibers as biomedical materials. The mechanical properties

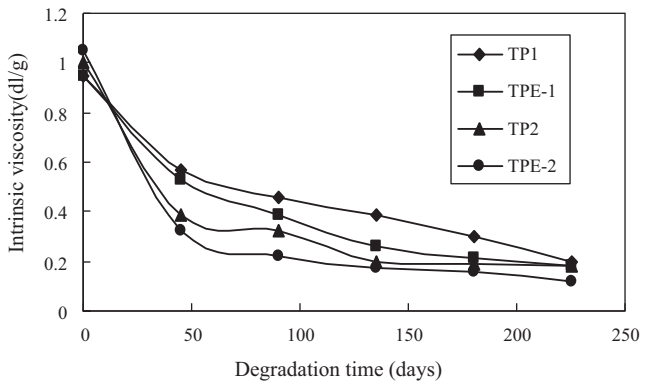

Fig. 4. The intrinsic viscosity of the electrospinning fibers and the corresponding membranes with degradation time.

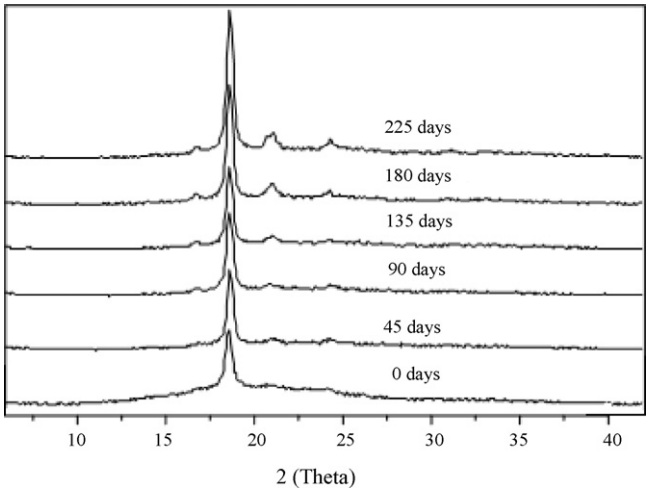

Fig. 5. XRD spectra of e-spun fibers TPE-1 with degradation time (days).

Table 2
Mechanical properties of electrospinning nanofibers.

Polymers	Tensile stress at maximum (MPa)	Tensile strain at maximum (%)
TP1	37.5	161
TPE-1	13.2	113
TP2	3.7	626
TPE-2	2.6	468

of nanofibers of CL/TMC/LLA tercopolymers were tested and listed in Table 2. Tensile stress at maximum of nanofibers was lower than that of corresponding copolymers. On one hand, the molecular chain orientation of single fiber improved with increasing the fiber elongation ratios during the electrospinning process. However, on the other hand, the disordered arrangement of nanofibers made its tensile strength decreased. In addition, the influence of the latter on the tensile strength was much higher than that of the former. Therefore, the tensile stress at maximum of nanofibers was lower than that of corresponding copolymers. The tensile stress at maximum of TPE-1 was higher than that of TPE-2, while the tensile strain at Maximum was opposite. The reason was also attributed to the different feed molar ratio of monomers in copolymers mentioned above. It was reported that the tensile fracture strength of human body skin was 5–30 MPa, elongation fracture was for 35–115%. Therefore, the prepared nanofibers have potential applications in biomedical field in view of the mechanical properties.

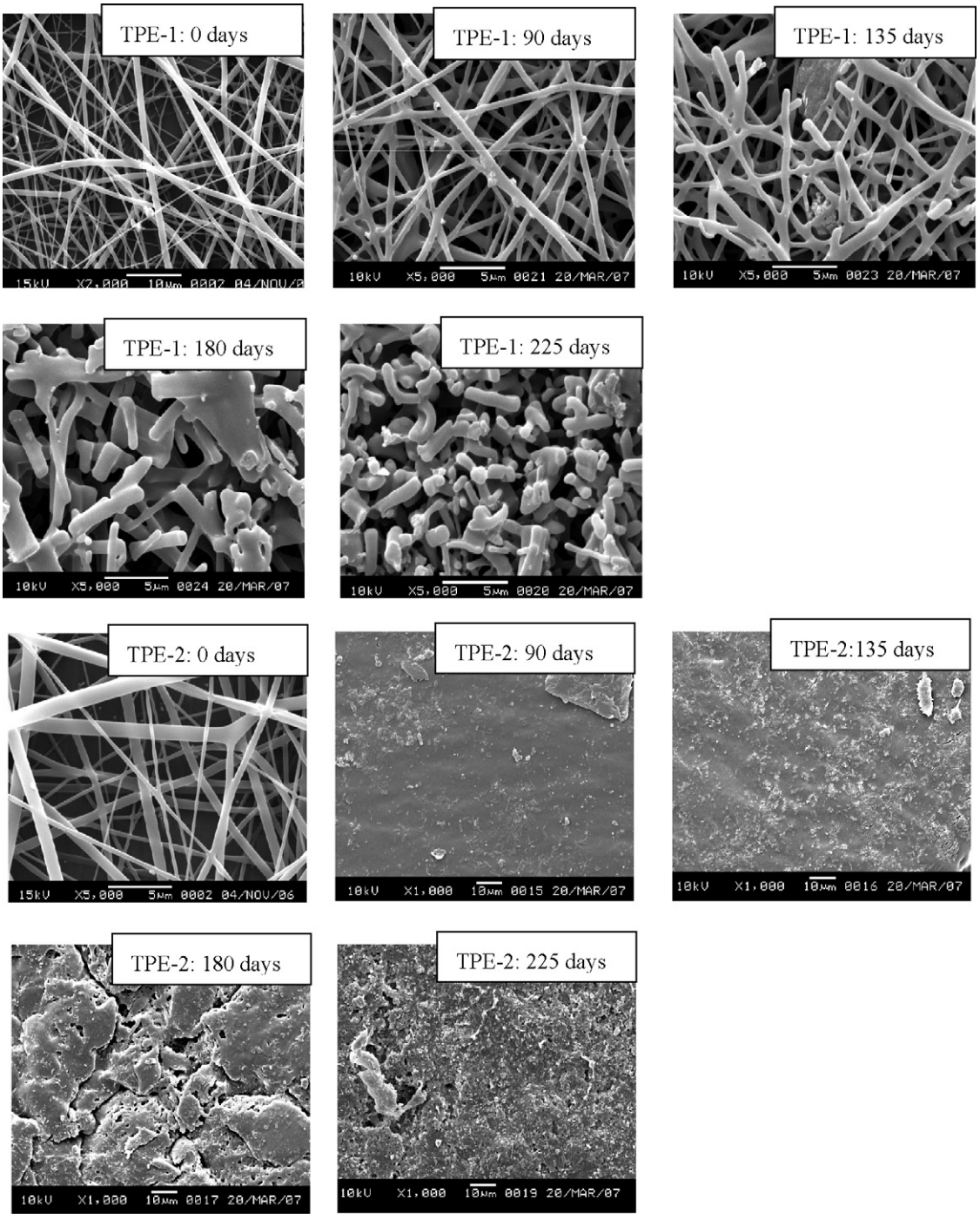

Fig. 6. SEM of TPE-1 and TPE-2 with degradation time.

3.3. Biodegradability

3.3.1. Viscosity changes

Fig. 4 shows the viscosity changes of the copolymer nanofibers with degradation time. The viscosity declined with increasing degradation time, which meant the degradation occurred with time. Compared the viscosity of the copolymer membranes with that of the corresponding nanofibers after degradation 225 days, it was found that the degree of viscosity decline of the former was littler than that of the latter. The phenomenon mentioned above was caused by large surface area to volume ratio of nanofibers, which offset the degradation effect of crystallinity and had a dominant position, though the crystallinity of nanofibers being higher than that of the corresponding copolymers.

3.3.2. XRD

Fig. 5 shows XRD spectra of TPE-1 with degradation time. It was obvious that the intensity of diffraction peak ($2\theta = 19^\circ$) of PLLA structural unit increased gradually with prolonging the degraded-time. After 45 days, the characteristic diffraction peaks ($2\theta = 21^\circ$ and 23°) for PLLA structural unit appeared, and the intensity of peaks strengthened with degradation time. Another diffraction peak ($2\theta = 17^\circ$) for PLLA was observed after 90 days, which followed the same rule mentioned above.

The biodegradation rate of PLLA is much faster than that of PCL and PTMC. The hydrolysis of aliphatic polyester first occurs in the amorphous area and the crystallization area edge. The ester bonds of polyester were attacked by water molecular, resulting in breaking of molecular chain and producing polymer pieces. These were verified by XRD spectra above.

3.3.3. SEM

Fig. 6 presents the SEM photos of TPE-1 and TPE-2 morphology in vitro with the degradation time. For TPE-1, a small amount of chippings scattered onto the fiber surfaces after 90 days, while the fiber morphology changed little. The fiber fracture could be seen obviously after 135 days, and the fracture further intensified with increasing time. After 225 days, the fibers became the short ones with the average length only about 2 μm, and looked like powder from the macroscopic view.

SEM photos of TPE-2 degradation morphology in vitro are very different from that of TPE-1. The fiber morphology has become vague and the membrane with holes could be seen after 90 days. The membrane with holes changed into the morphology with more holes and more blocks with prolonging the degradation time. After 225 days, the membrane morphology with more holes and more blocks evolved into crisp membrane with a lot of holes distributed on the surface of the membrane.

The phenomena could be interpreted as follows: LLA component in TPE-2 was lower than that of TPE-1, which made the sequence length of PLLA in molecular chain become short, resulting in T_g (5.2 °C) being much lower than the temperature of degradation (37 °C). Owing to heat effect in degradation conditions, the molecular chains slacked and fibers shrunk which caused fibers conglutination, and eventually formed adhesion membrane. The membrane was ruptured into blocks, which was caused by the strength loss of the membrane and the oscillating during degradation. In addition, due to CO_2 emission in degradation, many numerous holes formed in the surface of membranes. While for TPE-1, due to the high T_g, the degradation morphology of fiber was observed clearly during the whole degradation process.

4. Conclusions

The properties of ε-CL/TMC/LLA random tercopolymer nanofibers including the mechanical property and the thermal behavior, especially biodegradability, were investigated. Two melting points and a crystal exothermal peak were observed in the DSC curve of nanofiber. Due to stretching and molecular chain orientation in electrospinning process, the T_g, T_m and W_c of the nanofibers were higher than that of the corresponding tercopolymers. The T_g, T_m and W_c of the nanofibers decreased with increasing TMC content in copolymers. The mechanical properties of nanofibers changed with the different feed molar ratio. The degree of degradation of nanofibers was faster than that of the corresponding copolymers. In addition, the degradation behavior of nanofibers also altered with the different feed molar ratio. The data obtained would provide more details for application of tercopolymer nanofibers in biomedical field.

Acknowledgement

The project was financially supported by the Guangdong Natural Science Foundation (Project No. 10152902001000014)

References

Aussawasathien, D., Teerawattananon, C., & Vongachariya, A. (2008). Separation of micron to sub-micron particles from water: Electronspun nylon-6 nanofibrous membranes as pre-filters. *Journal of Membrane Science*, *315*, 11–19.

Duda, A., & Biela, T. (1998). Block and random copolymers of ε-caprolactone. *Polymer Degradation and Stability*, *59*, 215–220.

Fay, F., & Linossier, I. (2006). Degradation and controlled release behavior of ε-caprolactone copolymers in biodegradable antifouling coating. *Biomacromolecules*, *7*, 851–857.

Han, J., Branford-White, C. J., & Zhu, L.-M. (2010). Preparation of poly(ε-caprolactone)/poly(trimethylene carbonate) blend nanofibers by electrospinning. *Carbohydrate Polymers*, *79*, 214–218.

Jia, Y., & Dong, F. (2010). Preparation and characterization of biodegradable tercopolymers and their nano-structured fibers via electrospinning. *AATCC Review*, *4*, 49–50.

Jia, Y.-T., & Kim, H.-Y. (2006). Electrospun nanofibers of block copolymer of trimethylene carbonate and ε-caprolactone. *Journal of Applied Polymer Science*, *99*, 1462–1470.

Jia, Y., & Shen, X. (2008). Synthesis and characterization of tercopolymers derived from ε-caprolactone, trimethylene carbonate and lactide. *Polymers for Advanced Technologies*, *19*, 159–166.

Kim, K., & Yu, M. (2003). Control of degradation rate and hydrophilicity in electrospun non-woven PLA nanofibers scaffolds for biomedical application. *Biomaterials*, *24*, 4977–4985.

Kricheldorf, H. R., & Kreiser-Saunders, I. (1995). Polylactones: Sn(II) octoate-initiated polymerization of L-lactide: A mechanistic study. *Polymer*, *36*, 1253.

Laleh, G., & Molamma, P. (2008). Electrospun PCL/gelatin nanofibrous scaffolds for nerve tissue engineering. *Biomaterials*, *34*, 4532–4539.

Lee, K. Y., & Jeong, L. (2009). Electrospinning of polysaccharides for regenerative medicine. *Advanced Drug Delivery Reviews*, *61*, 1020–1032.

Li, W.-J., & Cato, T. (2002). Electrospun nanofibrous structure: A novel scaffold for tissue engineering. *Journal of Biomedical Materials Research*, *60*, 613–621.

Middleton, J. C., & Tipton, A. J. (2000). Synthetic biodegradable polymers as orthopedic devices. *Biomaterials*, *21*, 2335–2346.

Narayan, B., & Park, S. J. (2003). Synthesis and characterization of ABA type tri-block copolymers derived from p-dioxanone, L-lactide and poly(ethylene glycol). *Polymer International*, *520*, 6–14.

Rujitanaroj, P., & Pimpha, N. (2008). Wound-dressing materials with antibacterial activity from electrospun gelatin fiber mats containing silver nanoparticles. *Polymer*, *49*, 4723–4732.

Shen, Y. Q., Shen, Z. Q., Zhang, Y. F., Huang, Q. H., Shen, L. F., Yuan, H. Z., et al. (1997). Random copolymerization of ε-caprolactone and trimethylene carbonate with rare earth catalysts. *Journal of Applied Polymer Science*, *64*, 2131–2138.

Tsuji, H., & Ikada, Y. (1998). Blends of aliphatic polyesters. II. Hydrolysis of solution-cast blends from poly(L-lactide) and poly(ε-caprolactone) in phosphate-buffered solution. *Journal of Applied Polymer Science*, *67*, 405–415.

Xie, J. W., & Wang, C. H. (2006). Electronspun micro- and nanofibers for sustained delivery of paclitaxel to treat C6 glioma in vitro. *Pharmaceutics Research*, *23*, 1817–1825.

Yoo, H. S., & Park, T. G. (2009). Surface-functionalized electronspun nanofibers for tissue engineering and drug delivery. *Advanced Drug Delivery Reviews*, *61*, 1033–1042.

Zhu, K. J., & Pitt, C. G. (1991). Synthesis, properties and biodegradation of poly(1,3-trimethylene carbonate). *Macromolecules*, *24*, 1736–1741.

Zong, X., & Kim, K. (2002). Structure and process relationship of electrospan bioabsorbance membranes. *Polymer*, *43*, 4403–4412.